Supporting Information

Electrochemical energy storage in organic supercapacitor via a non-electrochemical proton charge assembly

Sanchayita Mukhopadhyay,[a] Alagar Raja Kottaichamy,[a,d] Mruthyunjayachari Chattanahalli Devendrachari,[a] Rahul Mahadeo Mendhe,[a] Harish Makri Nimbegondi Kotresh,*[b] Chathakudath Prabhakaran Vinod,*[c] and Musthafa Ottakam Thotiyl*[a]

[a] Department of Chemistry and Centre for Energy Science, Indian Institute of Science Education and Research, Pune, Dr. Homi Bhabha Road, Pune 411008, India.
E-mail: musthafa@iiserpune.ac.in

[b] Department of Chemistry, Acharya Institute of Technology, Soldevanahalli, Bangalore 560107, India.
E-mail: harishmnk@acharya.ac.in

[c] Catalysis and Inorganic Chemistry Division, CSIR-NCL, Pune 411008, India.
E-mail: cp.vinod@ncl.res.in

[d] Department of Chemistry and Ilse Katz Institute for Nanoscale Science and Technology, Ben-Gurion University of the Negev, Beer-Sheva 8410501, Israel.

1. Experimental:

1.1. Materials:

Phthalimide (99%), trimellitic anhydride (97%), cobalt (II) chloride hexahydrate (≥98%), copper (II) chloride dihydrate (≥98%), ammonium molybdate (99.99 %), ammonium chloride (≥98%), urea (99%), nitrobenzene (99%), ethanol (95%), isopropyl alcohol (99%), potassium hydroxide (99.98 %), sodium sulfide nonahydrate and dimethyl formamide (DMF) (99 %) were obtained from Alfa Aesar, India. The YP-50 was purchased from Kuraray

chemicals. Hydrochloric acid (HCl) (37.0 %), sulfuric acid (H_2SO_4) and Nafion solutions (5 wt. %) were received from Sigma Aldrich, India.

1.2. Synthesis:

1.2.1. Synthesis of CoPc and TCCoPc molecules:

The synthesis of the molecules was done by following reported procedures.[1-3] Cobalt (II) phthalocyanine (CoPc) and tetra carboxylic acid cobalt (II) phthalocyanine (TCCoPc) molecules were synthesised by mixing stoichiometric amount of cobalt (II) chloride hexahydrate (1.2 g), urea (7.5 g), ammonium chloride (0.5 g) and ammonium molybdate (0.05 g) along with phthalimide and trimellitic anhydride (3.98 g) for CoPc and TCCoPc respectively. The mixture was refluxed at 170–180 °C for 5 h after mixing with 30 mL of nitrobenzene in a round bottom flask. Thorough washing of the product obtained was carried out with ethanol and water to ensure no excess amount of urea is present. The product was purified by heating at 100^{o}C in an aqueous solution of KOH (0.1 M) and HCl (0.1 M) solution alternatively. Finally, the product was dried in a vacuum oven at ~80^{o}C overnight after multiple rinsing with ethanol and water to remove any excess acid or alkali impurity present.

1.2.2. Synthesis of CuPc, TCCoPc, TNCoPc and TACoPc molecules:

For the synthesis of copper (II) phthalocyanine (CuPc) and tetra carboxylic acid copper (II) phthalocyanine (TCCuPc) molecules above procedure was followed just by replacing cobalt (II) chloride hexahydrate with copper (II) chloride dihydrate. The tetra nitro cobalt (II) phthalocyanine (TNCoPc) molecule was also synthesised following the same procedure with 4-nitro phthalimide as the precursor in place of phthalimide. The tetra amino cobalt (II) phthalocyanine molecule was synthesised by reduction of the TNCoPc molecule. 0.75g of TNCoPc along with 3g of sodium nonahydrate and around 30mL of DMF were heated to 80^{o}C for ~ 2 hours in a round bottom flask. Following this ~ 200mL of dilute ice water was added into the mixture and the resulting precipitate was thoroughly washed with hot water, methanol and hexane. Finally, the precipitate was dried in an oven overnight to obtain TACoPc molecule.

1.2.3. Synthesis of CoPc and TCCoPc integrated with YP-50:

The composite of CoPc and TCCoPc with YP-50 was prepared by sonicating a known amount of both the phthalocyanine molecules with the YP-50 support in a stoichiometric weight ratio of 2:1 in N, N-dimethyl formamide (DMF) for 30 minutes. A well-mixed suspension was obtained which was further stirred at 80°C for ~ 24 hours. Following that the mixture was centrifuged and the resulting precipitate obtained was thoroughly washed with DMF and ethanol multiple times. Finally, the precipitate was dried overnight to get the final composite product.[4,5]

1.3. Methodologies:

1.3.1. Materials Characterization:

Matrix-assisted laser desorption ionization time-of-flight (MALDI-TOF-MS) mass spectrometry was carried out with AB SCIEX 4800 Plus TOF/TOF instrument. UV-Visible, Fourier transform infrared (FTIR) and Raman spectroscopic measurements of the molecules as well as the molecules integrated with YP-50 (composites) were carried out with the Perkin Elmer Lambda 950, Bruker Alpha ATR-FTIR and LabRAM HR, Horbia Jobin Yvon spectrometer respectively for all the systems. Zeiss Ultraplus-4095 instrument was used to carry out the scanning electron microscopy (SEM) with energy dispersive X-ray (EDX) measurement. X-ray photo electron spectroscopy (XPS) was carried out using Thermo Scientific Kalpha+ spectrometer. The measurements were carried out using a monochromatic Al Kα (1486.6 eV) X-ray source (72 W power) with a spot size of 400 µm. For electron energy analysis, a 180^{o} double focusing hemispherical analyzer with 128 channel detector was used. An ultralow energy co-axial electron beam and Ar+ ion beam was used for charge compensation. The final spectra were cross verified for charge accumulation with C1s standard value at 284.6 eV. The base pressure of the spectrometer was always better than ~5x10^{-9} mbar and ~1x10^{-7} mbar during data acquisition with flood gun on. The survey scan was collected at 200 eV pass energy and individual core-levels at 50 eV. Peak fitting was carried out using XPS Peak Fit software with a smart background.

1.3.2. Quartz Crystal Microbalance studies:

For understanding the pristine behavior of the molecules, the electrochemical measurements were also carried out by forming a monolayer of CoPc and TCCoPc molecules on glassy carbon electrodes. The formation and surface coverage of the monolayers were confirmed by the Quartz Crystal Microbalance (QCM) studies. QCM measurements were done in a flow cell mode. Carbon coated quartz resonator (9.120 MHz) was used as the base crystal. A 0.5 mM molecular catalyst solution in dimethyl formamide (DMF) was passed at a flow rate of 1 mL/min. Firstly, to get a stable background signal, DMF solution was flowed for 2 hours. Then in order to ensure the formation of the monolayer on the crystal, the solution of the molecules was circulated through it for around 7 hours continuously. Finally, to remove any weakly adsorbed molecular system on the surface of the crystal, fresh DMF solution was passed again for 2 hours. To find the mass of adsorbed molecules on the crystal surface, Sauerbrey equation (Equation S1) was used:

$$\Delta m = -c(\Delta f/n) \qquad \text{(S1)}$$

where, Δf is the net resonance frequency shift due to adsorption of molecules. The sensitivity (c) of the QCM crystal was 5.608 ng $cm^{-2}Hz^{-1}$. The surface coverage (Γ, $mol.cm^{-2}$) was calculated using equation S2,

$$\Gamma = \frac{\Delta m}{\text{molecular mass}} \qquad \text{(S2)}$$

1.3.3. Electrochemical Measurements (three electrode configuration):

Biologic VMP 300 was used for carrying out the electrochemical experiments. A three-electrode cell set up was used where the cell volume was 20 mL. A glassy carbon electrode having area 0.071 cm^2 was used as the working electrode, an $Ag/AgCl/Cl^-$ (3.5 M KCl) was used as the reference electrode and a Pt mesh was used as the counter electrode. The potentials were converted to reversible hydrogen scale (RHE scale) based on the H_2 reduction/oxidation reaction on a Pt disk electrode. The electrochemical investigations were done in 0.5 M sulfuric acid medium with CoPc and TCCoPc modified glassy carbon disk electrode. Drop casting method was used for the preparation of the electrodes. At first a homogenous dispersion of the system (composite of phthalocyanine molecule with YP-50) was prepared by sonicating a known amount of the composite material in isopropyl alcohol with 5 wt % Nafion as the binder

for an hour. Following that the prepared ink was drop casted on the glassy carbon disk electrode which was cleaned each time by polishing with 0.005 µm alumina powder followed by electrochemical cycling in the supporting electrolyte.

1.3.4. Supercapacitor Measurements (two electrode configuration):

Two-electrode cells consisted of composite (CoPc@YP-50 and TCCoPc@YP-50) electrode and an activated carbon (AC) counter electrode. The device was assembled into two electrodes split test cell (MTI Cooperation, USA). The composite electrodes were fabricated using carbon paper (AvCarb MGL190) as the current collector. The counter AC electrode fabrication was carried out by mixing 95 wt.% AC and 5 wt.% of Nafion binder manually in isopropyl alcohol until a homogenous ink was obtained. The ink was coated onto carbon paper sheets with a thickness of ~ 0.15 mm as supercapacitor electrodes (1.4 cm diameter), with a mass loading of ~ 7 mg/cm². Two-electrode split test cell was assembled according to established protocols.[6,7] Briefly, with the molecular system a circular composite electrode (1.4 cm diameter) was fabricated with a mass loading of nearly 3.5 mg/cm^2. These electrodes were stacked with a glass fiber filter paper separator (thickness = 0.20 mm) wetted with 400 µL of 0.5 M H_2SO_4 aqueous electrolyte. The stack was enclosed in a split test cell and assembled with silicone O ring rubber to prevent electrolyte evaporation and short circuiting.

2. Calculations:

2.1. Specific capacitance calculation (Csp):

The specific capacitance (Csp) was calculated from cyclic voltammetry (CV) curves (in three electrode configurations) at various scan rates using the following equation S3.[8-10]

$$Csp = \frac{\int i\ dV}{2 \times m \times \nu \times \Delta V} \qquad (S3)$$

where, Csp is specific capacitance is in (F/g), ∫i.dV is the integrated area in the cyclic voltammogram, m is the mass of the active material (g), v is the scan rate (V s^{-1}) and ΔV is the

voltage window (V). The Csp from the galvanostatic charge-discharge (GCD) measurements (in three electrode configurations) was calculated using the equation S4.

$$Csp = \frac{I \times \Delta t}{m \times \Delta V} \qquad (S4)$$

where Csp is specific capacitance (F/g), I is applied current (A), ΔV represents the potential window (V), Δt signifies discharge time (s) and m is the mass of the active material (g).

2.2. Capacitive contributions analysis:

The capacitive contribution to the current response can be obtained by analysing the cyclic voltammograms. The current response at different potentials is expressed as being the combination of surface capacitive effects and diffusion-controlled processes.[11] The capacitive effects were characterized by analyzing the cyclic voltammetry data at various sweep rates as per equation S5. Plot of $i/v^{1/2}$ vs. $v^{1/2}$ for both the molecules will provide the non-faradaic and faradaic contributions at various potentials. In equation S5, $k_1 v$ and $k_2 v^{1/2}$ correspond to the current contributions from the surface capacitive effects and the diffusion-controlled process, respectively. Thus, by determining k_1 and k_2, it is possible to quantify, the current fraction arising out of these contributions. The capacitive currents (orange shaded regions) and diffusion currents (green shaded regions) as demonstrated in Fig. 2b and Fig. 2c are determined from the total current using equation S5.

$$i(V) = k_1 v + k_2 v^{1/2} \qquad (S5)$$

3. Results:

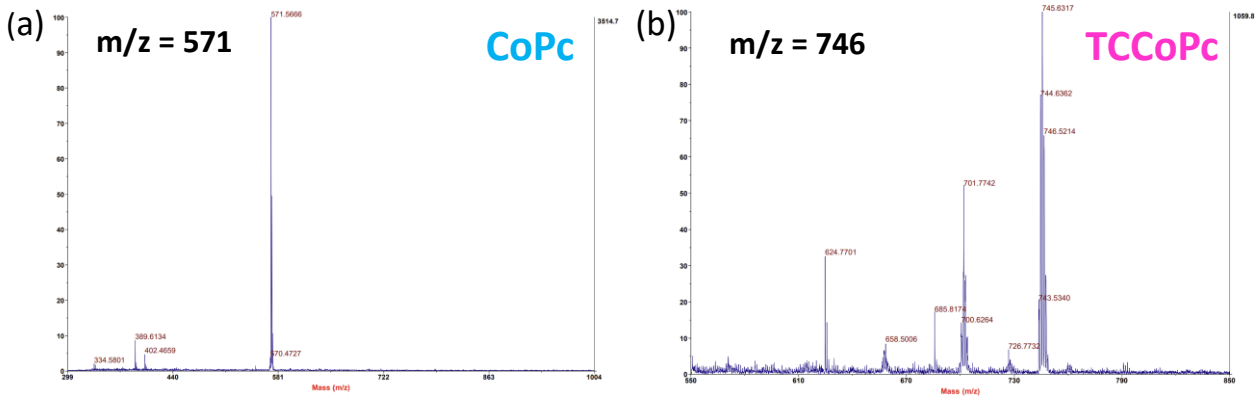

Fig. S1 Matrix-assisted laser desorption ionization time-of-flight mass spectrometry (MALDI-TOF-MS) of (a) CoPc and (b) TCCoPc molecules.

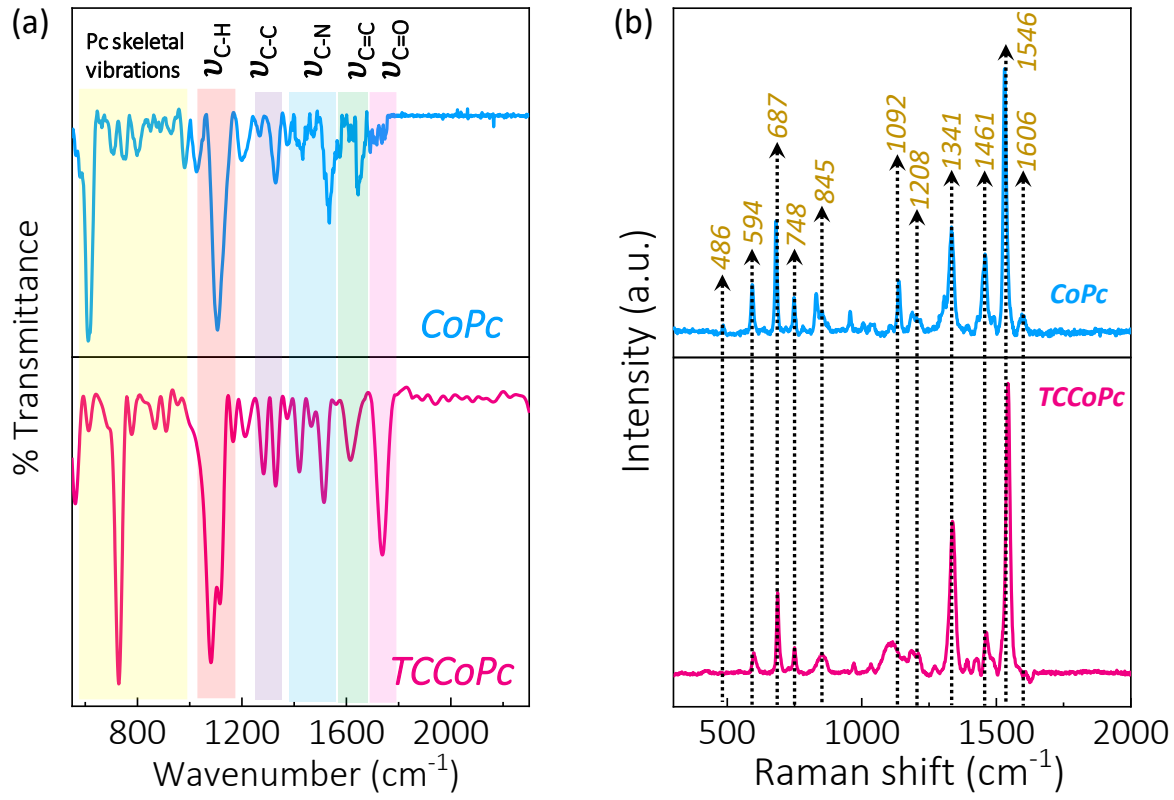

Fig. S2 (a) FT-IR and (b) Raman spectra of CoPc and TCCoPc molecules.

Table S1 Allotment of spectral peaks observed in the Raman spectra of CoPc and TCCoPc.

Raman shift (cm^{-1})	Band corresponding to
486	In plane bending of C-C-C
687	Out of plane bending of pyrrole ring
748	Macrocyclic stretching
845	Benzene breathing
1092	C-H bending
1208	In plane deformation of C-H
1341	In plane stretching of C-N
1461	Isoindole ring stretching
1546	In plane stretching of macrocycle
1606	In plane stretching of C-N

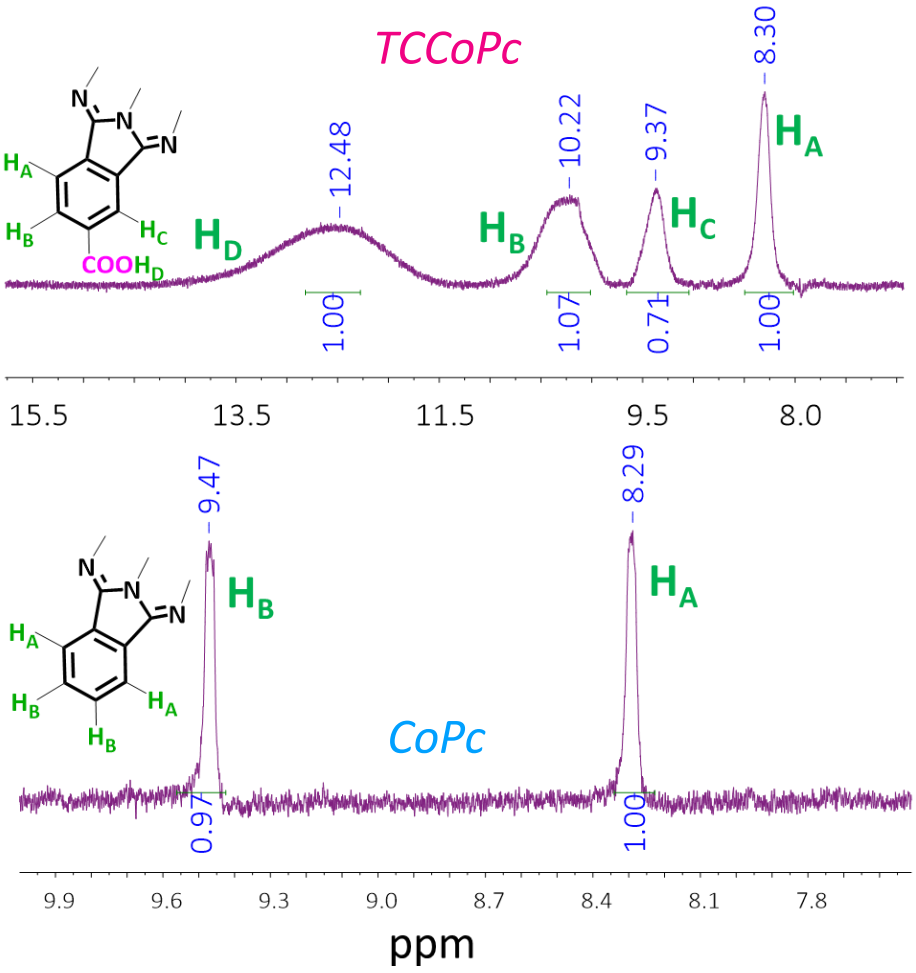

Fig. S3 ^{1}H NMR spectra of CoPc and TCCoPc molecules.

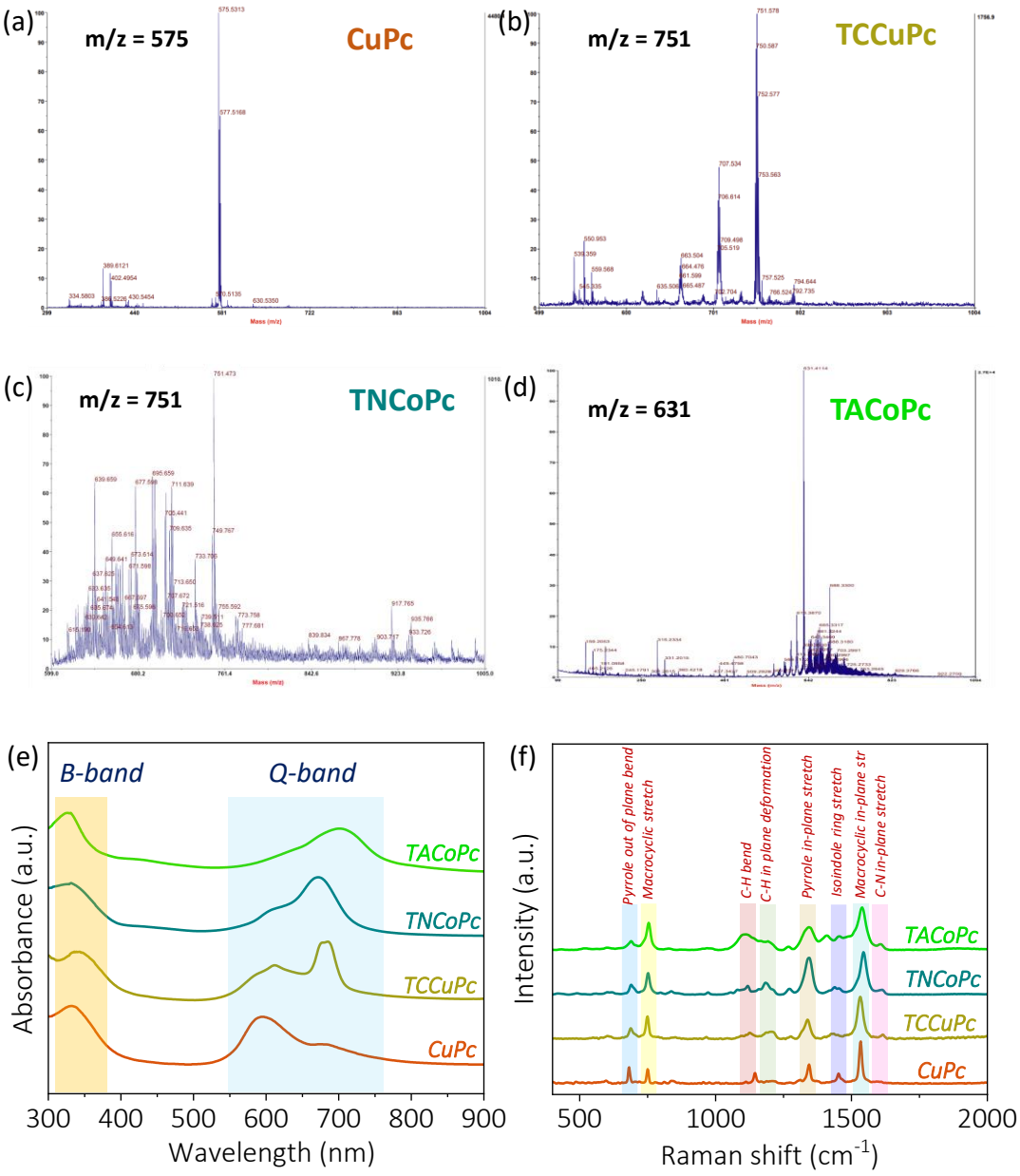

Fig. S4 (a-d) MALDI, (e) UV-visible and (f) Raman spectra of CuPc, TCCuPc, TNCoPc and TACoPc molecules.

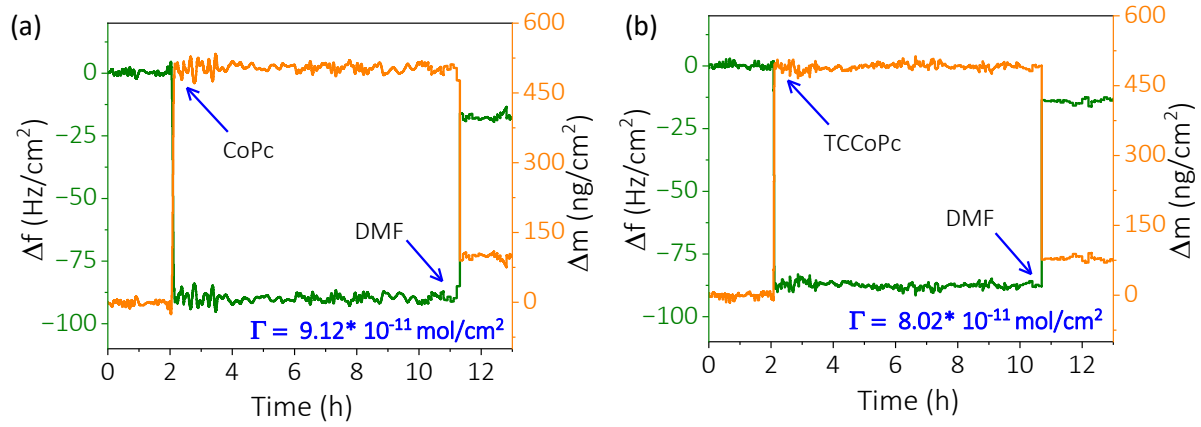

Fig. S5 Quartz crystal microbalance (QCM) measurement data of CoPc and TCCoPc molecules on a quartz resonator (carbon coated) during the adsorption of the molecules. (a) CoPc (0.5 mM) and (b) TCCoPc (0.5 mM) in dimethyl formamide (DMF). Green trace corresponds to the frequency change during adsorption and the orange trace corresponds to the mass change calculated using Saurbrey equation. Surface coverage (Γ) values of the molecules are provided in each graph.

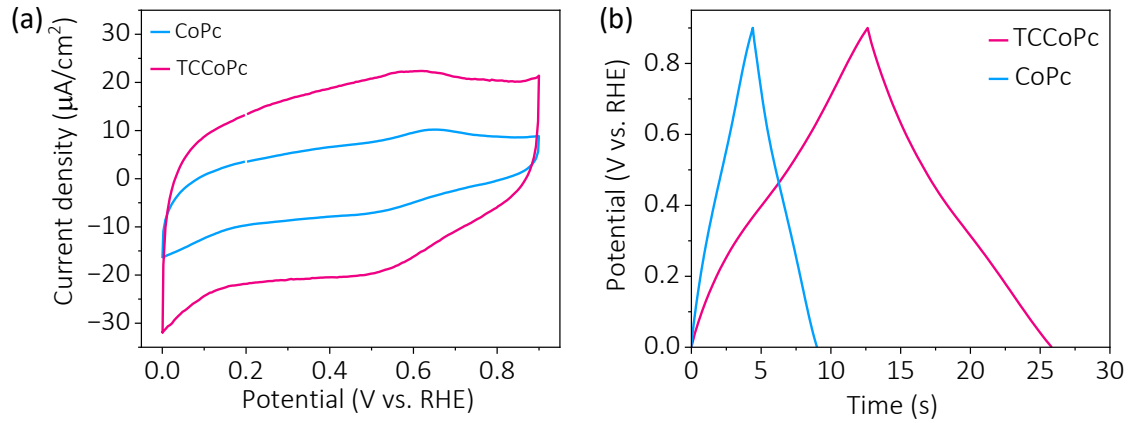

Fig. S6 (a) Cyclic voltammogram of CoPc and TCCoPc molecules adsorbed as monolayer on a GC electrode at a scan rate of 5 mV/s. (b) Galvanostatic charge discharge of CoPc and TCCoPc molecules adsorbed as monolayer on a GC electrode at 0.1 mA/cm^2.

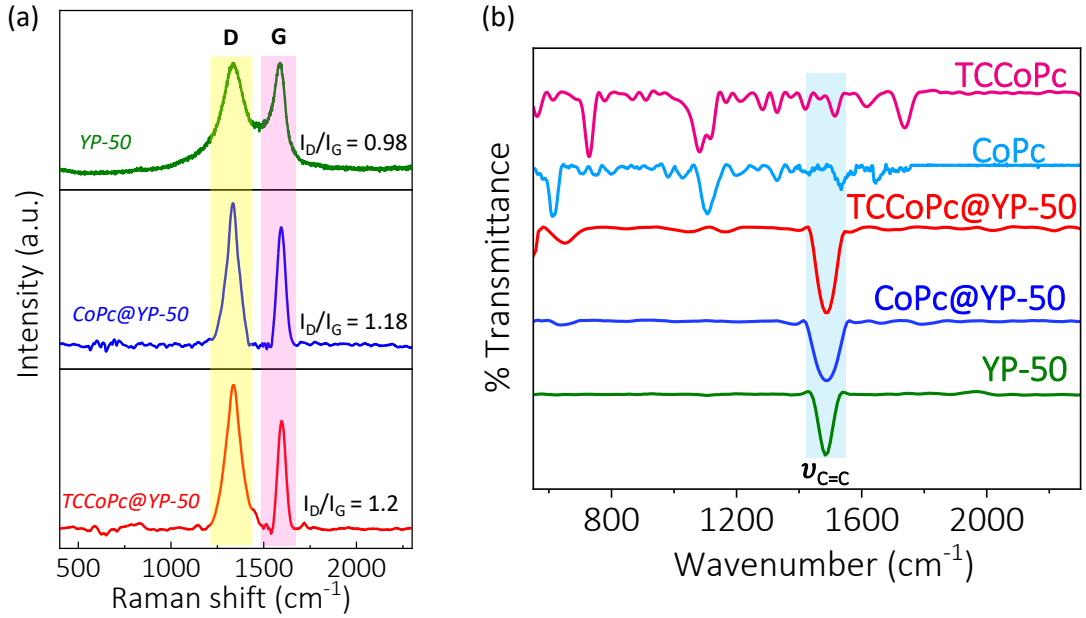

Fig. S7 (a) Raman spectra and (b) FT-IR spectra of YP-50, CoPc@YP-50 and TCCoPc@YP-50 composite systems.

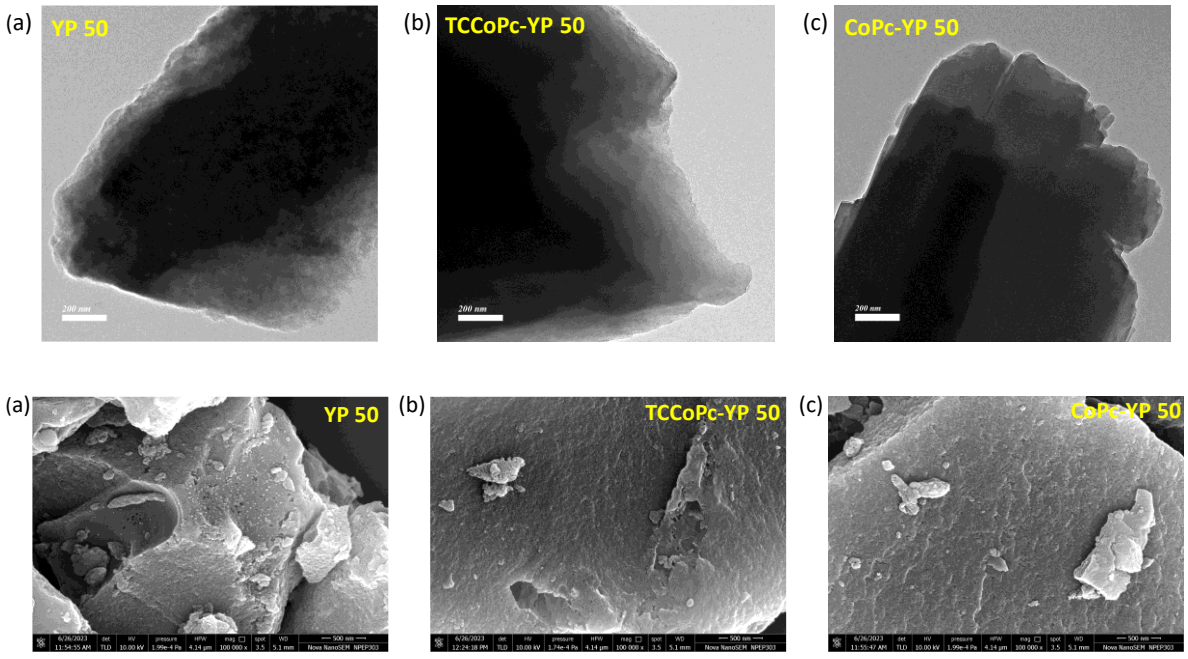

Fig. S8 HRTEM (top panel) and FESEM (bottom panel) images of (a) YP-50, (b) TCCoPc@YP-50 and (c) CoPc@YP-50.

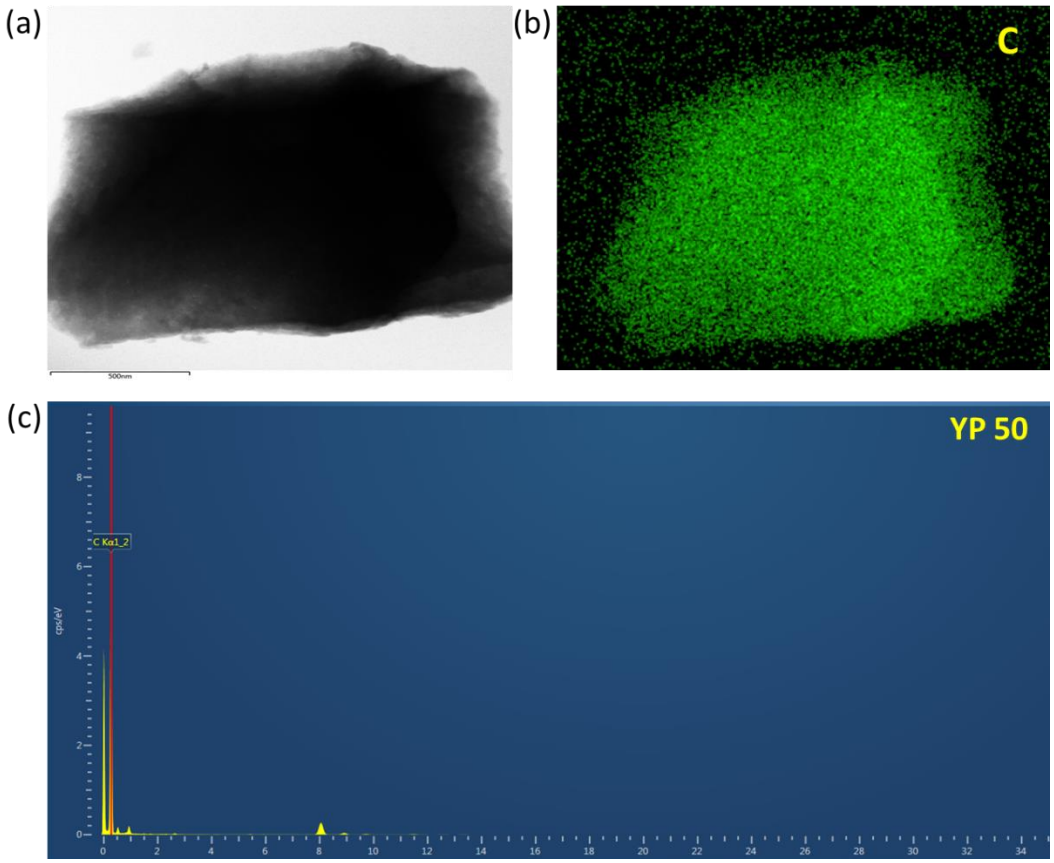

Fig. S9 HRTEM image along with elemental mapping and EDX of YP-50.

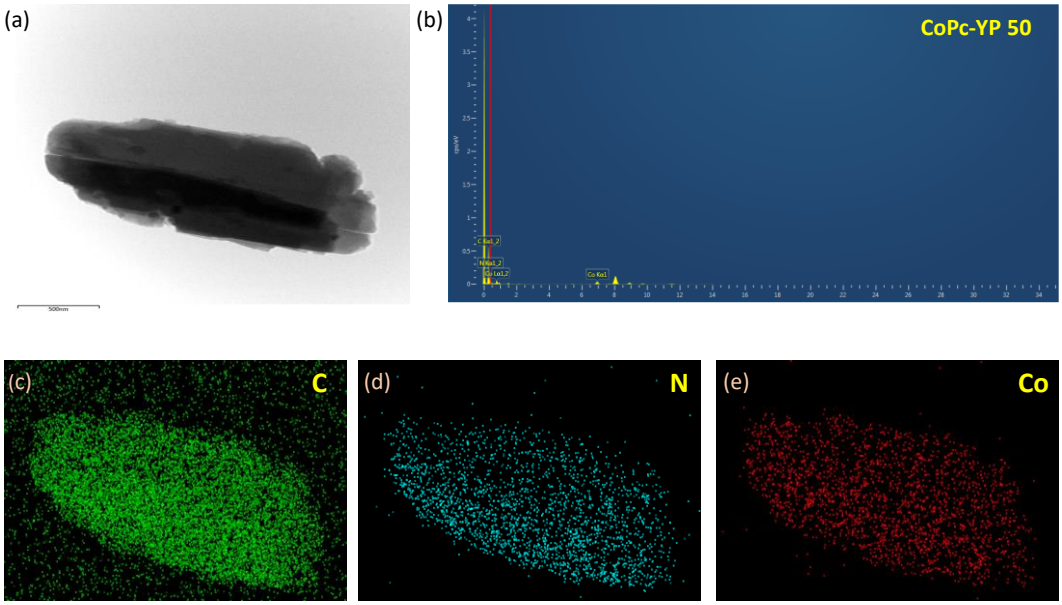

Fig. S10 HRTEM image along with elemental mapping and EDX of CoPc@YP-50.

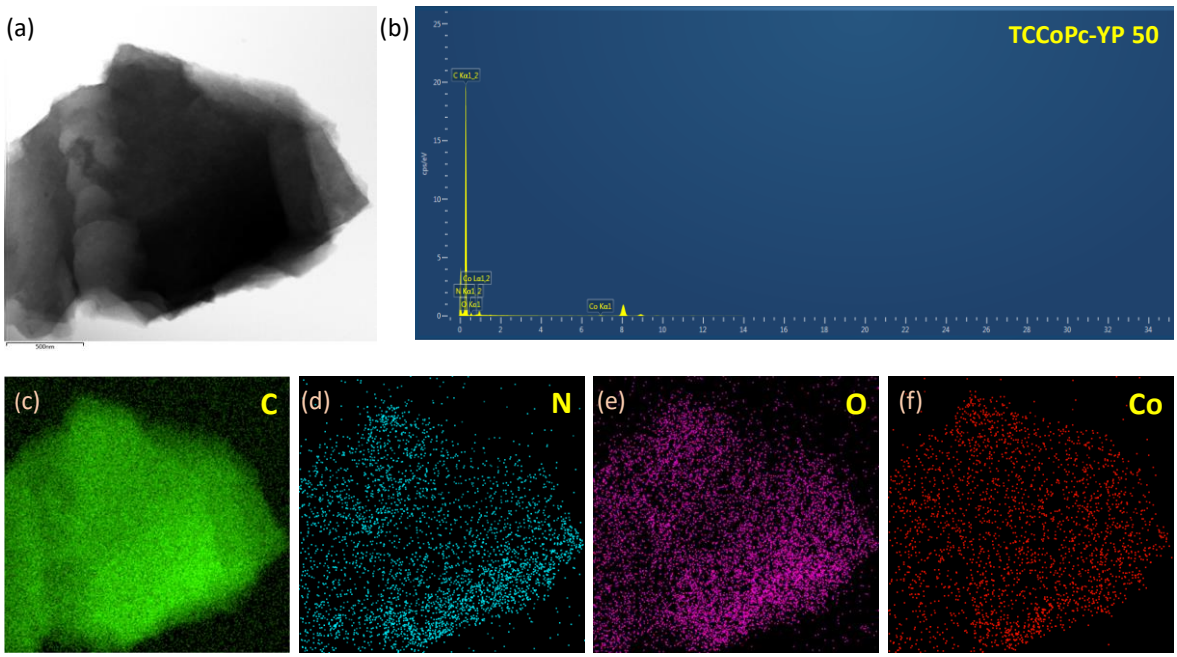

Fig. S11 HRTEM image along with elemental mapping and EDX of TCCoPc@YP-50.

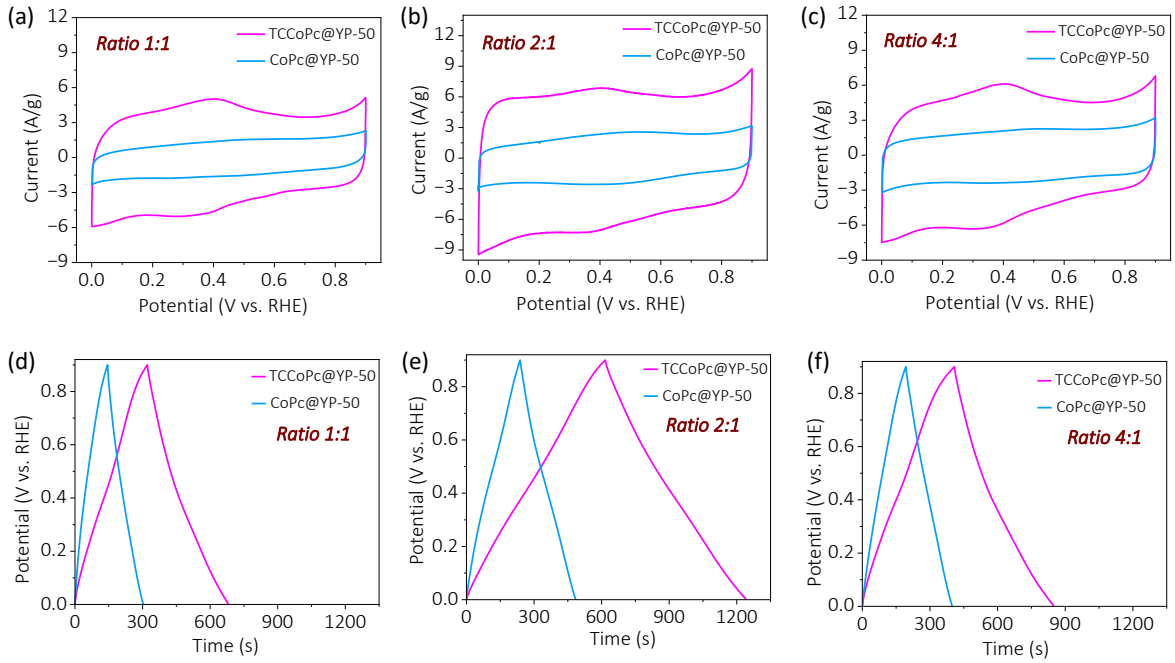

Fig. S12 (a-c) Cyclic voltammetry at a scan rate of 5 mV/s and (d-f) galvanostatic charge-discharge profiles (at 1 A/g rate) for 1:1 (YP-50 to CoPc/TCCoPc), 2:1 (YP-50 to CoPc/TCCoPc) and 4:1 (YP-50 to CoPc/TCCoPc) weight ratio composition.

Table S2 Specific capacitance for different weight ratios of CoPc and TCCoPc composites with YP-50. The parameters are extracted from Fig. S12.

Ratio of composite (YP-50 : CoPc/TCCoPc	From cyclic voltammetry Csp (F/g)		From Galvanostatic charge-discharge Csp (F/g)	
	CoPc@YP-50	TCCoPc@YP-50	CoPc@YP-50	TCCoPc@YP-50
1:1	136	388	169	402
2:1	233	682	269	715
4:1	205	454	219	483

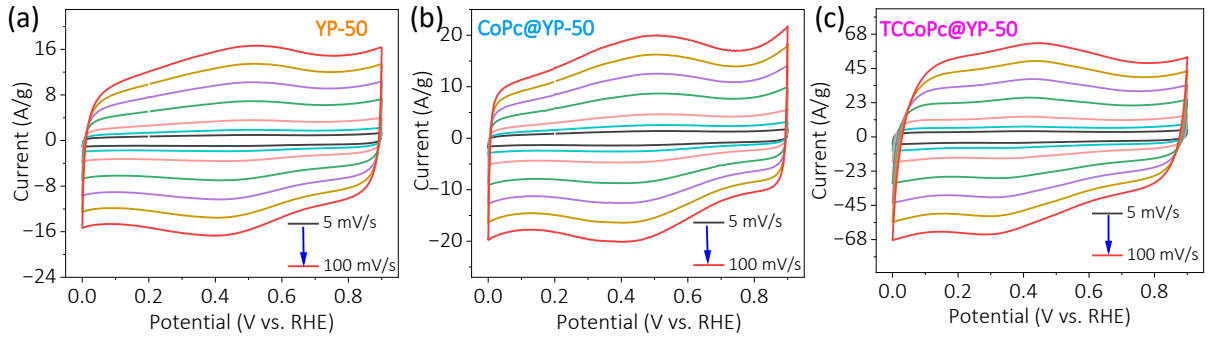

Fig. S13 Cyclic voltammograms at various scan rates from 5 mV/s to 100 mV/s for (a) YP-50, (b) CoPc@YP-50 and (c) TCCoPc@YP-50.

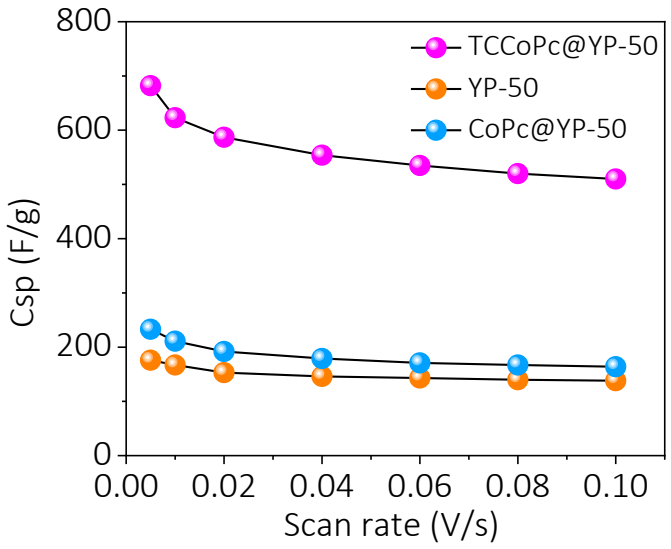

Fig. S14 Rate profile extracted from the cyclic voltammograms at various scan rates from 5 mV/s to 100 mV/s for YP-50, CoPc@YP-50 and TCCoPc@YP-50.

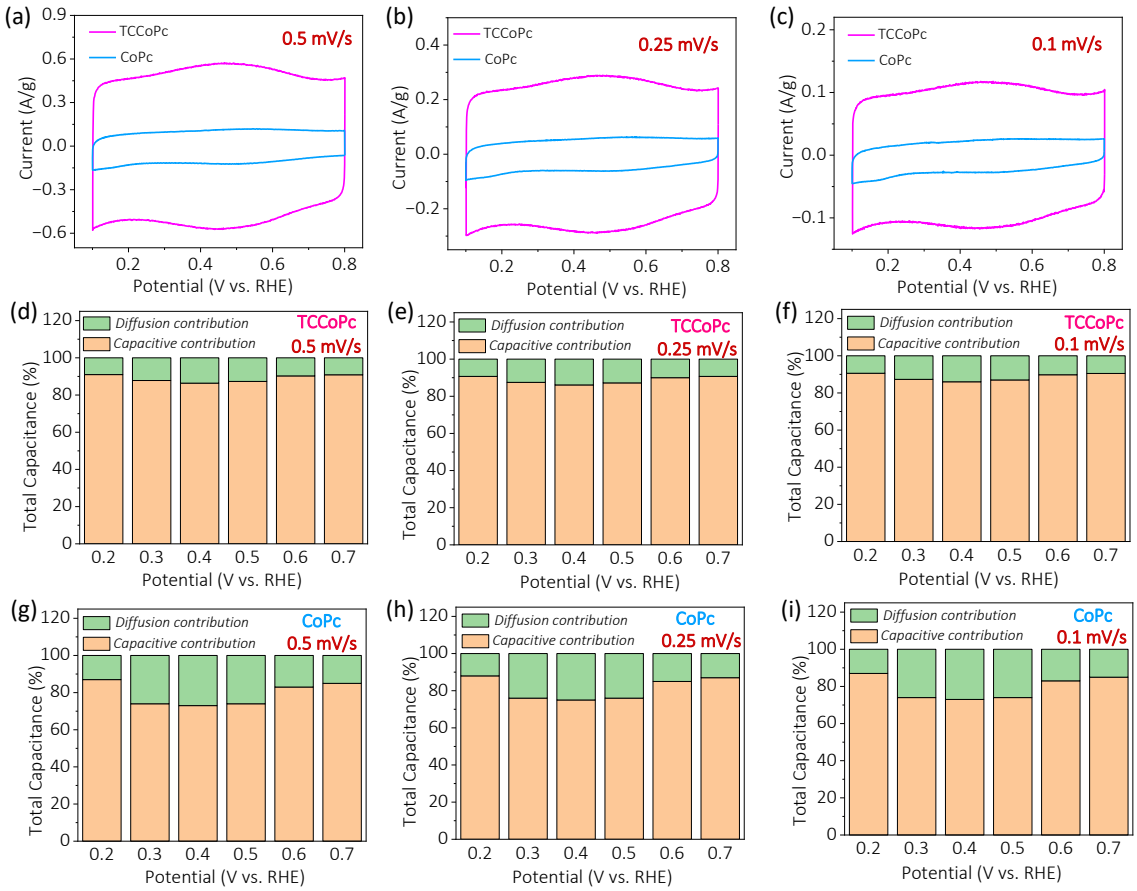

Fig. S15 (a-c) Cyclic voltammograms of CoPc and TCCoPc from 0.5 mV/s to 0.1 mV/s. Histogram plots demonstrating the percentage of capacitive and diffusional contributions at 0.5 mV/s, 0.25 mV/s and 0.1 mV/s scan rates for (d-f) TCCoPc and (g-i) CoPc molecules respectively.

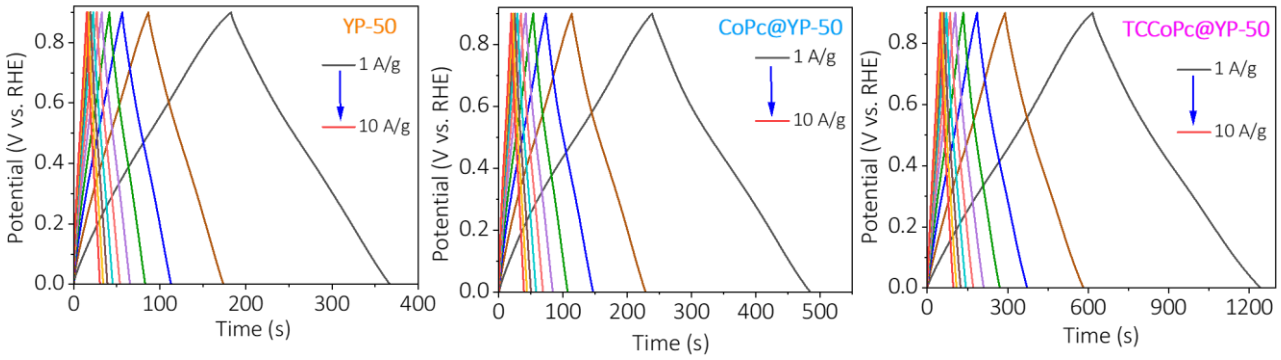

Fig. S16 Galvanostatic charge-discharge at various rates for (a) YP-50, (b) CoPc@YP-50 and (c) TCCoPc@YP-50.

Table S3 Specific capacitance (Csp) extracted from the cyclic voltammogram at 5 mV/s and galvanostatic charge-discharge at 1 A/g for YP-50, CoPc@YP-50 and TCCoPc@YP-50 composites.

Composite electrodes	**From Cyclic Voltammetry Csp (F/g)**	**From Galvanostatic charge-discharge Csp (F/g)**
YP-50	176	204
CoPc@YP-50	233	269
TCCoPc@YP-50	682	715

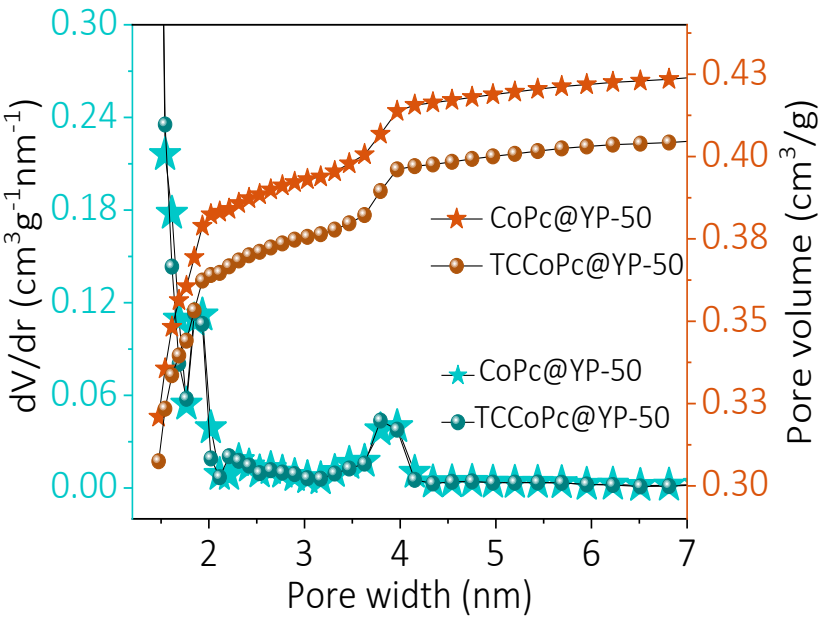

Fig. S17 Pore size distribution plot by DFT method extracted from BET analysis for CoPc@YP-50 and TCCoPc@YP-50.

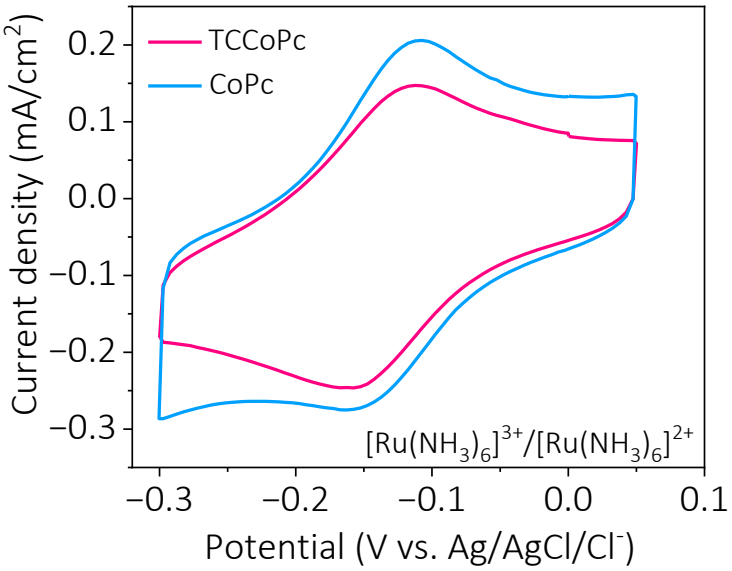

Fig. S18 Cyclic voltammograms for 5 mM $[Ru(NH_3)_6]^{2+}$ in 0.5 M H_2SO_4 medium collected at a scan rate of 20 mV/s with CoPc and TCCoPc molecules.

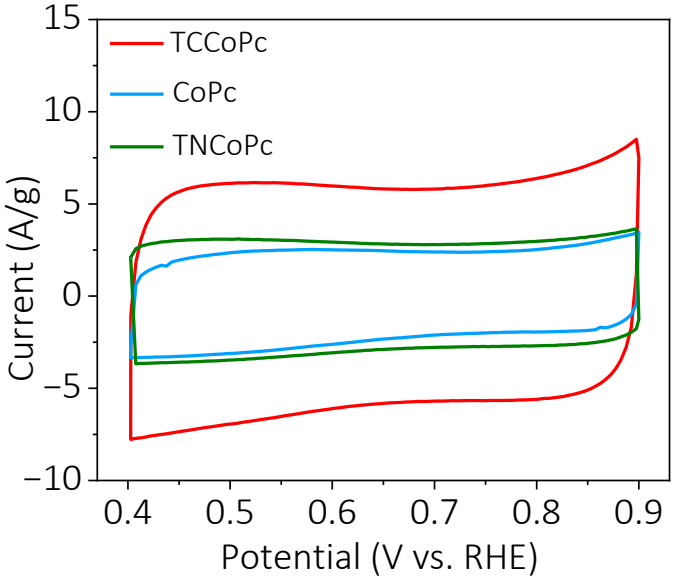

Fig. S19 Comparison of cyclic voltammograms at a scan rate of 5 mV/s for CoPc, TNCoPc and TCCoPc molecules in acidic medium.

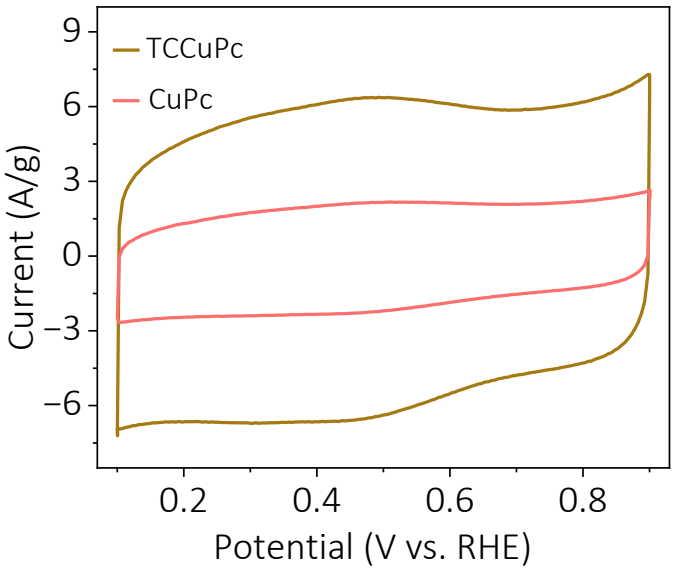

Fig. S20 Comparison of cyclic voltammograms at a scan rate of 5 mV/s for CuPc and TCCuPc molecules in acidic medium.

Table S4: Specific capacitance (Csp) extracted from the cyclic voltammogram at 5 mV/s for CoPc, CuPc, TCCoPc and TCCuPc molecules in acidic medium.

Electrode material	Csp (F/g)
CoPc	233
CuPc	211
TCCoPc	682
TCCuPc	657

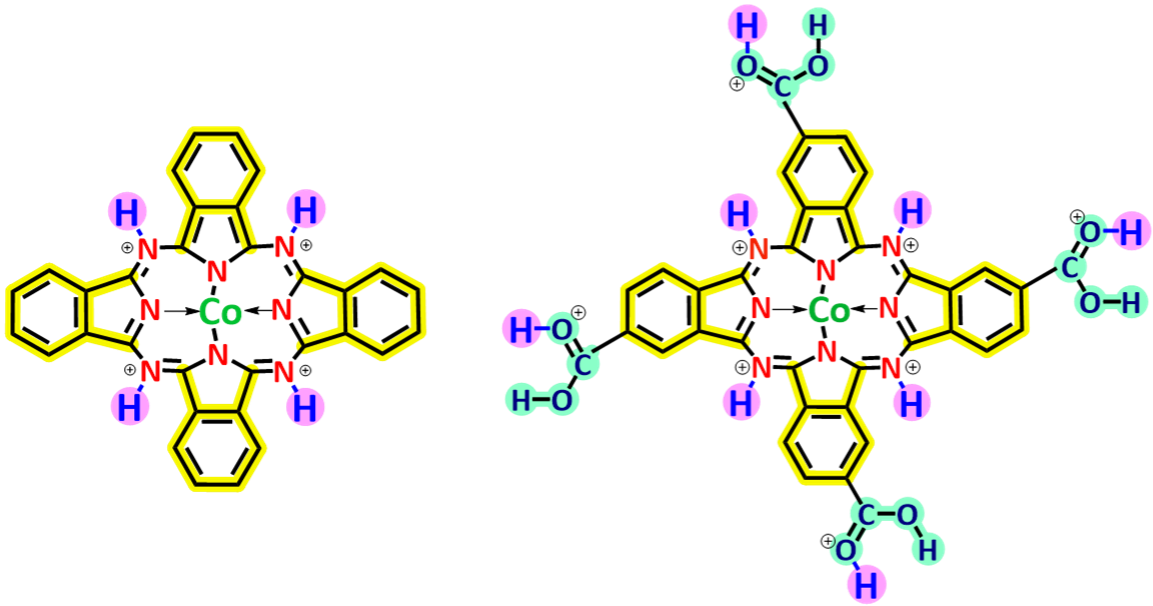

Scheme S1 Schematic illustration of proton charge assembly in CoPc and TCCoPc molecules in acidic medium.

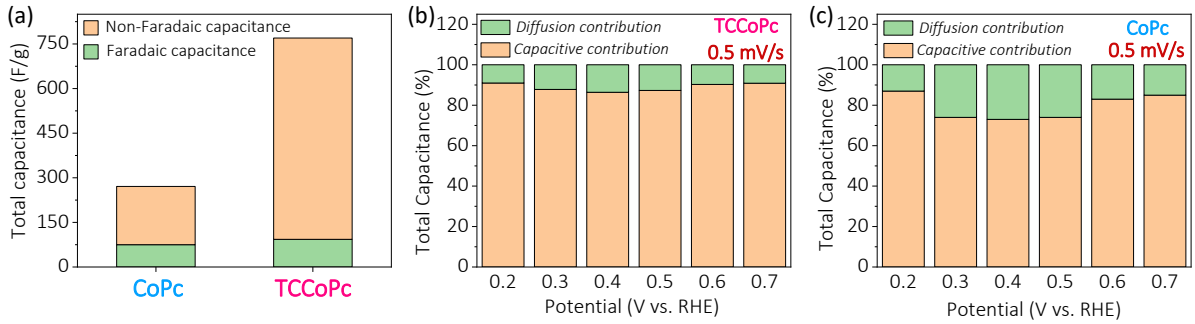

Fig. S21 Histogram plot showing (a) Faradaic and non-Faradaic contributions with respect to total specific capacitance for CoPc and TCCoPc at 0.4 V. The percentage contribution of Faradaic and non-Faradaic capacitance in (b) TCCoPc molecule and (c) CoPc molecule.

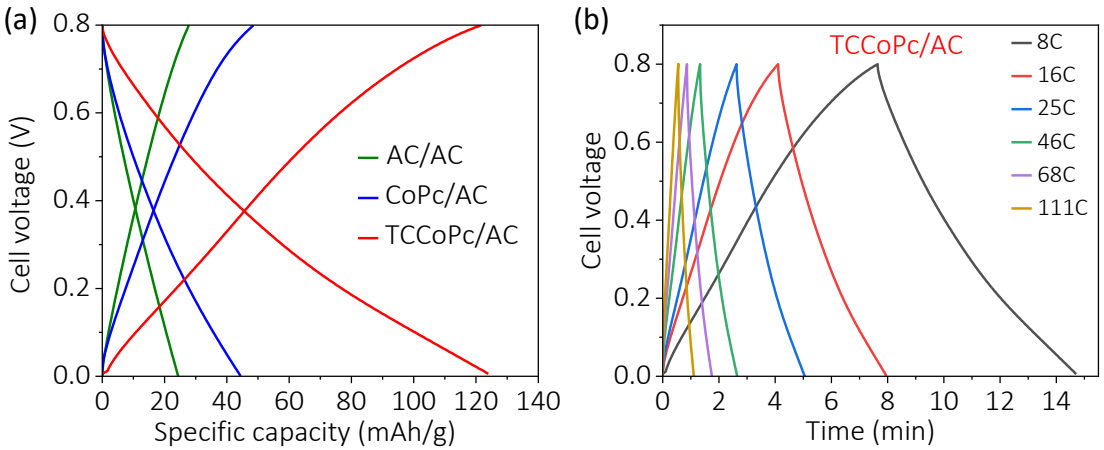

Fig. S22 (a) Comparison of specific capacity of all the three composite electrodes at a current rate of 1A/g and (b) Galvanostatic charge discharge of TCCoPc/AC at various rates.

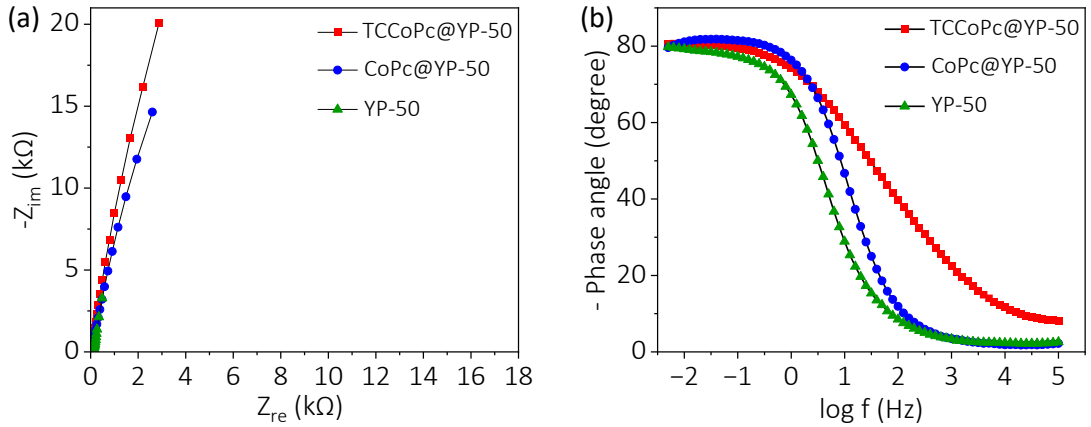

Fig. S23 (a) Nyquist plots and (b) Bode plots for YP-50, CoPc@YP-50 and TCCoPc@YP-50 electrodes at 0 V vs. OCV. The plots were acquired in the frequency range of 100 kHz to 5 mHz with a 10 mV AC excitation signal.

Table S5 Knee frequency and relaxation time for YP-50 and its composite electrodes determined using the electrochemical impedance spectroscopy (EIS) method.

Composite electrodes	**Knee frequency (f_0) in Hz**	**Time constant (τ_0) in ms**
YP-50	3	333
CoPc@YP-50	10	100
TCCoPc@YP-50	49	20.4

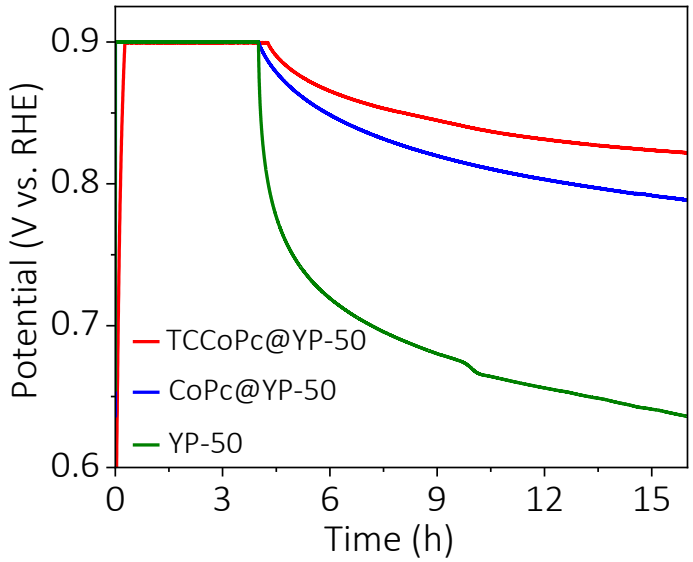

Fig. S24 Self-discharge profiles of YP-50, CoPc@YP-50 and TCCoPc@YP-50 in a three-electrode configuration as detailed in the experimental section.

Table S6 Self-discharge current and leakage current values extracted from Fig. S24.

Electrode Materials	**TCCoPc@YP-50**	**CoPc@YP-50**	**YP-50**
Specific capacitance (F/g)	715	269	204
Self discharge current (µA)	18.10^{-3}	26.10^{-3}	35.10^{-3}
Leakage current (mA/F/V)	77.10^{-3}	139.10^{-3}	192.10^{-3}

Table S7 Comparison of specific capacitance, specific energy and specific power of different phthalocyanine based supercapacitors (in three electrode configurations).

System	Electrolyte	Current rate (A/g)	Specific capacitance (F/g)	Specific Energy (Wh/kg)	Specific Power (W/kg)	References
NiPc NF-rGO	1M H_2SO_4	1	223	15	350	Appl. Surf. Sci., 2018, **449**, 528–536
CuPcTs-Ppy/ MWCNT	3M H_2SO_4	5	488	67.7	2500	Electrochim. Acta, 2018, **265**, 594–600
N-CuMe2Pc-GO	1M H_2SO_4	0.5	291.6	32.8	225	Electrochim. Acta, 2019, **298**, 770–777
Cu(II)Pc/acid activated MWCNT/Ppy	1M H_2SO_4	10	304	42	4973	Int. J. Energy Res., 2020, **44**, 9093–9111
CoPc@CNTs	6M KOH	1	1112	55.6	300	J. Mol. Liq., 2022, **359**, 119319
$Co(NO_2)_4$Pc-rGO	1M H_2SO_4	4	150	20.8	1994	Synth. Met., 2023, **293**, 117284
ZnPc-400//Zn Zn-ion	1M $ZnSO_4$	1	164	86.2	220	Chem. Eng. J., 2023, **468**, 143875
TCCoPc@YP-50	0.5M H_2SO_4	1	715	80.4	450	**This work**

4. References:

1 A. K. Al-lami, N. N. Majeed and A. H. Al-mowali, *Chem. Mater. Res.*, 2013, **3**, 59.

2 C. Chen, Z. Ma, S. Zhou, T. Li, X. Sun, *Catal. Letters,* 2017, **147**, 2399–2409.

3 E. A. Lukyanets and V. N. Nemykin, *J. Porphyr. Phthalocyanines*, 2010, **14**, 1–40.

4 R. Cao, R. Thapa, H. Kim, X. Xu, M. G. Kim, Q. Li, N. Park, M. Liu and J. Cho, *Nat. Commun.*, 2013, **4**, 1–7.

5 S. Mukhopadhyay, A. R. Kottaichamy, Z. M. Bhat, N. C. Dargily and M. O. Thotiyl, *Electroanalysis*, 2020, **32**, 2387–2392.

6 T. I. Singh, G. Rajeshkhanna, T. Kshetri, N. H. Kim, J. H. Lee, *J. Mater. Chem. A*, 2020, **8**, 26158–26174.

7 H. Li, J. Lang, S. Lei, J. Chen, K. Wang, L. Liu, T. Zhang, W. Liu, X. Yan, *Adv. Funct. Mater.,* 2018, **28**, 1–12.

8 H. Wu, Z. Lou, H. Yang, G. Shen, *Nanoscale,* 2015,**7**, 1921-1926.

9 Q. Wang, X. Wang, J. Xu, X. Ouyang, X. Hou, D. Chen, R. Wang, G. Shen, *Nano Energy* 2014, **8**, 44–51.

10 J. Bae, M. K. Song, Y. J. Park, J. M. Kim, M. Liu, Z. L. Wang, *Angew. Chemie,* 2011, **123**, 1721–1725.

11 D. Bruce et al., *J. Phys. Chem. C,* 2007, **111**, 14925-14931.